Vujadin Aleksić
Srđan Bulatović ✉
Bojana Zečević
Ana Maksimović
Ljubica Milović

https://doi.org/10.21278/TOF.464041622
ISSN 1333-1124
eISSN 1849-1391

PROCESSING OF DATA OBTAINED BY THE TESTING OF STEEL UNDER LOW CYCLIC FATIGUE (PART I)

Summary

The design of mechanical components exposed to fatigue load, at a low number of cycles, requires knowledge of the behaviour of the material under the impact of variable load in conditions of controlled strain when cyclic plasticity is present. The aim of testing the quality of the material of the components exposed to low cycle fatigue (LCF) in many industries: nuclear, aerospace, mechanical, civil engineering and shipbuilding. In order to ensure the reliability and consistency of the results from different laboratories, it is necessary to collect all test data using test and data processing methodologies that are in accordance with a number of key points of ISO 12106: 2017 and/or ASTM E 606-04 standards. This paper defines a new data processing methodology after the LCF testing of steel.

Keywords: *stabilized hysteresis, low cycle fatigue (LCF), HSLA steel*

1. Introduction

European and American standards, ISO 12106:2017 (E) [1] and ASTM E 606-04 [2], define only the general methodology of the LCF testing of metals. These tests provide huge amounts of data (see Table 1). Fig. 1 graphically shows the LCF test data of the base metal (BM) of steel NN-70, high strength low-alloyed steel (HSLA), for only one amplitude level of regulated strain, $\Delta\varepsilon/2$, which needs to be filtered from a large amount of data needed to define the characteristic stabilized hysteresis.

The data of characteristic stabilized hysteresis, N_s, for each amplitude level of regulated strain define low-cycle fatigue curves, which describe the behaviour of steel under load conditions of low-cycle fatigue. The problem arises related to the objective and subjective impact in determining the stabilized hysteresis, and then regarding the measured and read values of the parameters that are further processed. This paper presents the methodology for determining the characteristic stabilized hysteresis, N_s, for each amplitude level of regulated strain (characteristic cycles) in LCF testing.

Table 1 Analysis of the large amount of data obtained by LCF testing of NN-70 steel

LCF NN-70		**File analysis**			**EXCEL data**			
Spec.	$\Delta\varepsilon/2$, %	File name	A4 format		Number of columns	Number of rows	Number of items of data	Total data
			Number of pages	File size KB				
09	0.35	OM-09-035_1od12_N=1do749	572	1492	7	32005	224035	**2385575**
		OM-09-035_2od12_N=750do1499	572	1502	7	32005	224035	
		OM-09-035_3od12_N=1500do2253	572	1490	7	32005	224035	
		OM-09-035_4od12_N=2254do2995	543	995	5	32005	160025	
		OM-09-035_5od12_N=2996do3738	572	1489	7	32005	224035	
		OM-09-035_6od12_N=3739do4481	572	1677	7	32005	224035	
		OM-09-035_7od12_N=4482do5224	572	1506	7	32005	224035	
		OM-09-035_8od12_N=5225do5967	572	1496	7	32005	224035	
		OM-09-035_9od12_N=5968do6710	572	1515	7	32005	224035	
		OM-09-035_10od12_N=6711do7453	572	1496	7	32005	224035	
		OM-09-035_11od12_N=7454do8196	572	1009	5	32005	160025	
		OM-09-035_12od12_N=8197do8429	179	316	5	9842	49210	
		Σ	**6422**	**15983**			**2385575**	
03	0.50	OM-03-050_1od3_N=1do742	582	991	5	32005	160025	**349050**
		OM-03-050_2od3_N=743do1485	582	990	5	32005	160025	
		OM-03-050_3od3_N=1486do1619	106	324	5	5800	29000	
		Σ	**1270**	**2305**			**349050**	
06	0.60	OM-06-060_1od1_N=1do655	480	867	5	27801	139005	**139005**
		Σ	**480**	**867**			**139005**	
08	0.80	OM-08-080_1od1_N=1do248	192	501	5	10544	52720	**52720**
		Σ	**192**	**501**			**52720**	
Σ		***17 files***	***8384***	***19656***			***2926350***	***2926350***

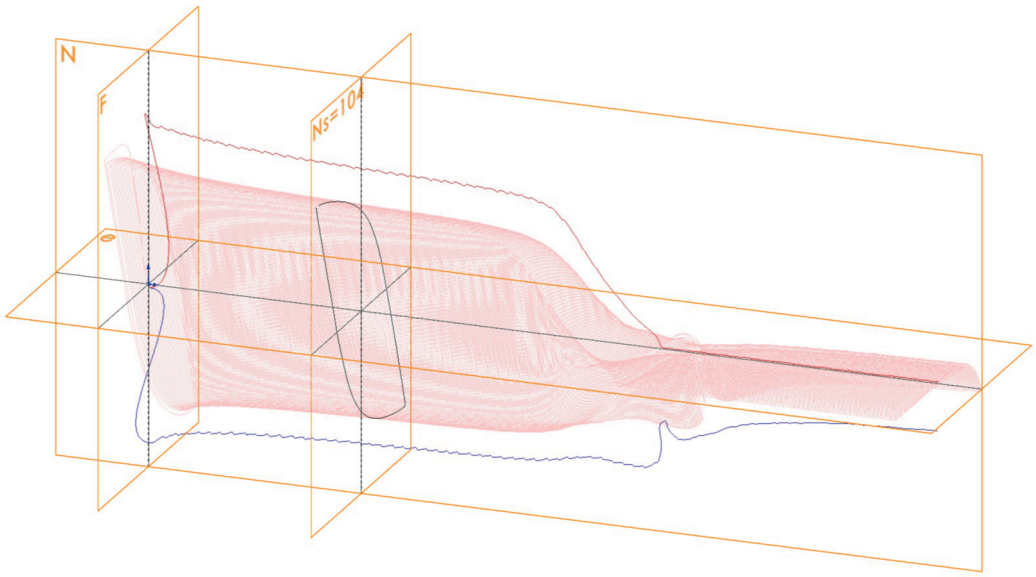

Fig.1 Large amount of data to be processed (Specimen 08, $\Delta\varepsilon/2$=0.80 %, from Table 1)

2. Failure criteria for the LCF testing of steel - Excerpt from standard ISO 12106: 2017

The failure criteria are usually based on the occurrence, presence or intensification of a phenomenon observed or recorded that indicates serious damage to or imminent failure of the sample. The number of cycles to failure, N_f, can be defined as the number of cycles that meet the following failure criteria:

a) complete separation of the sample into two different parts;

b) a certain percentage of change in the maximum tensile stress in relation to the level determined during the test;

c) a certain change in the ratio of the modulus of elasticity in the tension and pressure part of the hysteresis loop; most often, E_T/E_C = 0.5 is used to define failure (see Fig. 2a);

d) a certain percentage of change in the maximum tensile stress relative to the maximum tensile stress.

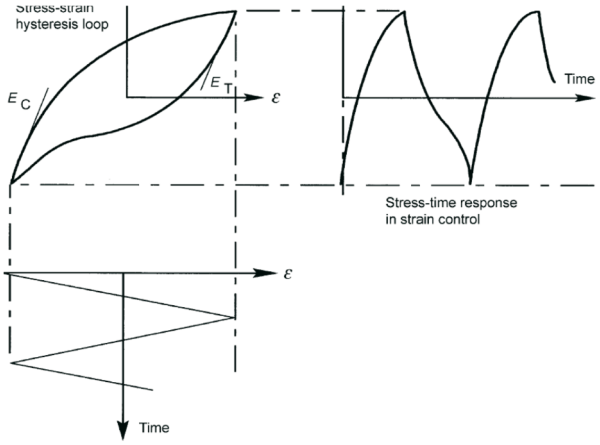

Figure 9 — Definitions of tension and compression modulus for determination of failure

a) definitions of tension and pressure modules for determining failure

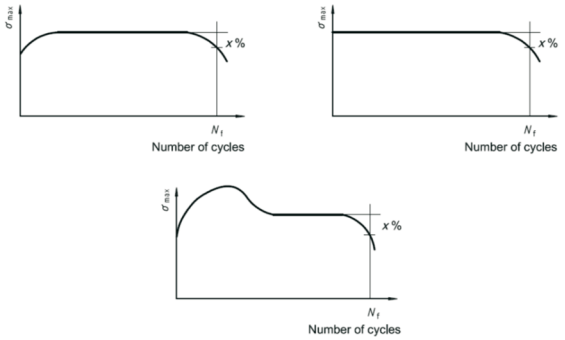

b) for materials with stable or steady-stable behaviour after initial hardening then softening

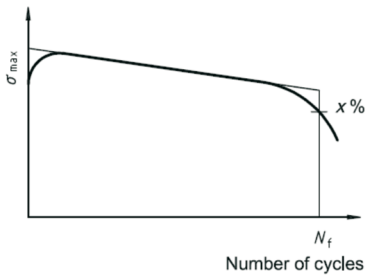

c) for materials with continuous softening

Fig. 2 Definitions of failure criteria

The use of criteria a) and b) is the most common and any of the above criteria can be used for failure. The report lists the specific failure criteria used for the series of tests. Fig. 2 (b and c) shows examples of stress reduction criteria. In this paper, the number of cycles that have to be applied to achieve a failure, N_f, is defined as the number of cycles corresponding to a stress reduction of x = 25% extrapolated over the tensile stress curve – the number of cycles when the stress drops sharply.

This criterion refers to the presence of one (or more) macroscopic cracks in the sample. In general, the ratio of the crack area to the original cross-sectional area of the sample is the same size as the stress reduction ratio.

3. LCF testing of steel

The behaviour of the material under low-cycle fatigue is tested experimentally, in accordance with ISO 12106: 2017 (E) [1] and/or ASTM E 606-04 [2]. For this purpose, smooth specimens are used which are exposed to low-cycle fatigue at several levels of regulated strain, with a cycle asymmetry factor, $R_\varepsilon = \varepsilon_{min}/\varepsilon_{max}$ = -1, at room, elevated, or reduced temperatures [3, 4]. The stress-strain response at low-cycle fatigue has the shape of idealized hysteresis loops [3-8] shown in Fig. 3. The strain range of strain $\Delta\varepsilon$ corresponds to the overall loop width, and the stress range $\Delta\sigma$ corresponds to its overall height. The stress amplitude is equal to the stress half-range, $\Delta\sigma/2$.

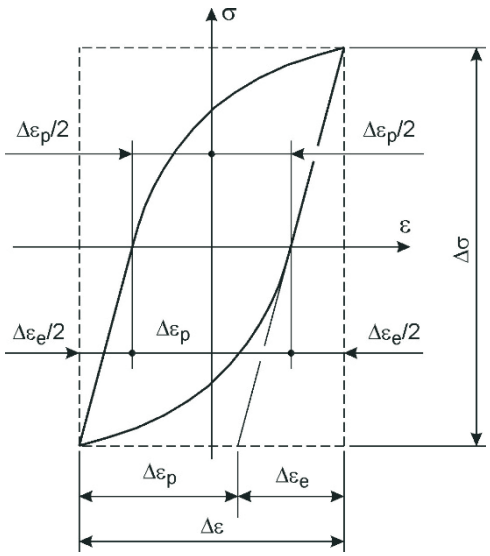

$\Delta\varepsilon_p/2$ – plastic strain amplitudes
$\Delta\varepsilon_e/2$ – elastic strain amplitudes

$\Delta\sigma = \Delta F/A_o$
σ – tension or compression stress in MPa
F – tensile or compressive load in kN
A_o – initial cross-section of the test specimen in mm^2

Fig. 3 Idealized hysteresis loop [3, 4]

Most materials, at low cyclic fatigue, achieve a so-called stabilized condition at a certain level of regulated strain. This is the condition when the height of the hysteresis loop expressed over the range of the load force or stress changes slightly and is called the stabilization area (Fig. 4a-d). For the analysis at R_ε = -1, it is sufficient to consider the positive part of the *F-N* curve (Fig. 4b) [9-24]. Detailed data (the shape, dimensions of the test specimen and regime of the controlled strain) have been presented in papers [9-15] in order to obtain a wider picture of the experiment which produced the results used in this paper.

The hysteresis for the N_s cycle in the stabilization region, which is close to or equal to half the number of cycles to crack initiation N_f, is called the characteristic stabilized hysteresis [3-8]. The choice of stabilized hysteresis from a wide range of stabilized hysteresis, which best characterizes the behaviour of the material for a certain level of strain, is very important. It is representative of all hysteresis and serves to describe the procedure of low-cycle fatigue loading. All necessary data are read by stabilized hysteresis to determine the characteristic curves of low-cycle fatigue, the cyclic stress-strain curve (CSSC) (Fig. 4c and Fig. 4e), and the basic curves of low-cycle fatigue (BCLCF) (Fig. 4d and Fig. 4f).

The standards do not define the method or methodology for determining the characteristic stabilized hysteresis, N_s, for each amplitude level of regulated strain.

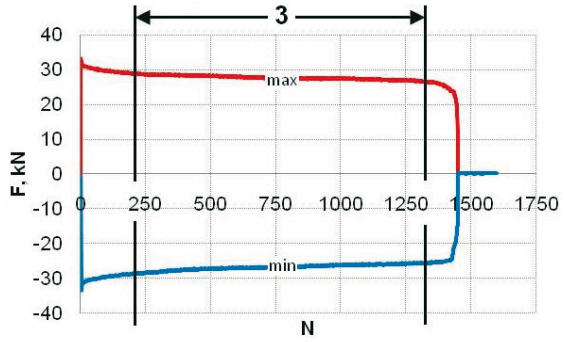

a) *F-N* curve, max-min, for one amplitude level of strain, Δε/2 [9,13]

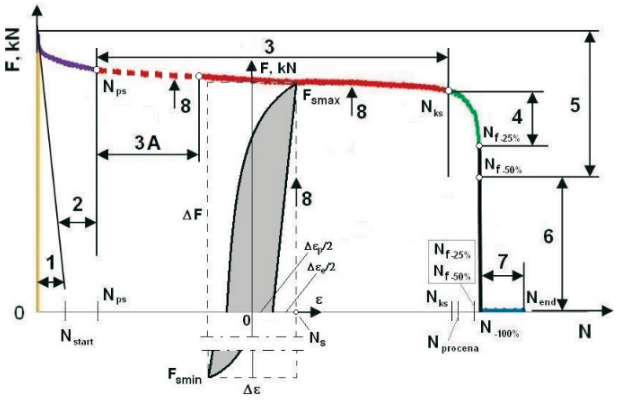

b) *F-N* curve, max only [9,13]

1 –Adjustment of tearing machine; 2 –Adjusting of tearing machine, tools and specimen; 3 –Stabilized state**;** 3A –Non-destructive testing (NDT) threshold; 4 –Force drop of 25% (ISO 12106: 2017 (E)) [1]; 5 –Force drop of 50% (ASTM E 606-04) [2]; 6–Force drop to $F = 0$; 7 –Stopping of tearing machine; 8 –Hysteresis loop height;

N_{start} – Test start up, F = max = F_{max}; N_{bs} –The beginning of stabilization; N_{es} – End of stabilization; $N_{fxx\%}$ – Force drop by xx%; $N_{estimation}$ – Force drop assessment of an operator; N_{end} –End of test.

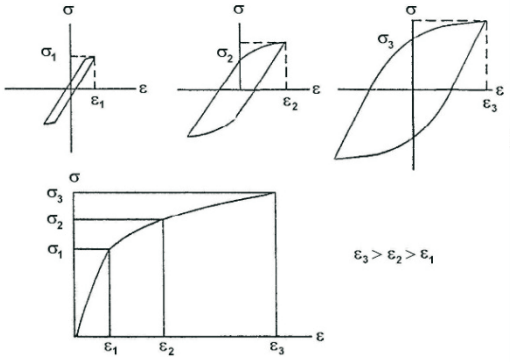

c) CSSC- cyclic stress-strain curve [25]

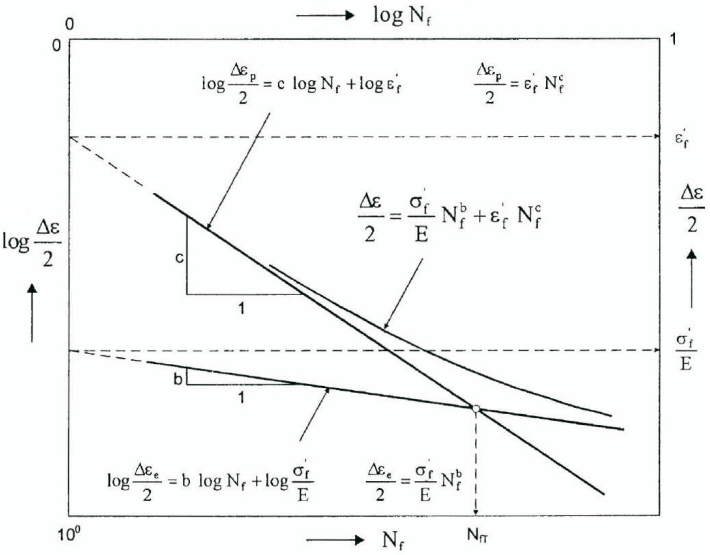

d) BCLCF- basic curves of low-cycle fatigue [3]

Property	Determination	Relation
$\sigma_{y'}$, cyclic yield strength (0,2 % offset)		
n', cyclic strain hardening exponent	Slope of lg σ_a = lg ε_{pa} plot	
K', cyclic strength coefficient	Stress intercept at ε_{pa} = 1 on lg σ_a – lg ε_{pa} plot	$\sigma_a = K'(\varepsilon_{pa})^{n'}$
Constitutive equation		$\frac{\Delta\varepsilon}{2} = \frac{\sigma_a}{E} + \left(\frac{\sigma_a}{K'}\right)^{1/n'}$

e) Table from the standard for defining CSSC [1]

Fig. 4 Initial and final test results of low-cycle fatigue steels

Property	Determination	Relation
$\sigma_{f'}$, fatigue ductility coefficient	Stress intercept at $2N_f = 1$ on lg σ_a – lg $2N_f$ plot	$\sigma_a = \sigma_{f'}(2N_f)^b$ (Basquin equation)
b, fatigue strength exponent	Slope of lg $(\Delta\varepsilon_e/2)$ – lg $2N_f$ plot (Specify $2N_f$ range)	
$\varepsilon_{f'}$, fatigue ductility coefficient	Plastic-strain intercept at $2N_f = 1$ on lg $(\Delta\varepsilon_p/2)$ – lg $2N_f$ plot	$\Delta\varepsilon_p/2 = \varepsilon_{f'}(2N_f)^c$ (Coffin-Manson equation)
c, fatigue ductility exponent	Slope of lg $(\Delta\varepsilon_p/2)$ – lg $2N_f$ plot (Specify $2N_f$ range)	
Total strain amplitude	$\Delta\varepsilon_t/2 = \Delta\varepsilon_e/2 + \Delta\varepsilon_p/2$ $\Delta\varepsilon_t/2 = (\sigma_{f'}/E)(2N_f)^b + \varepsilon_{f'}(2N_f)^c$	

f) Table from the standard for defining BCLCF [1]

Fig. 4 Initial and final test results of low-cycle fatigue steels (continued)

4. New LCF steel testing data processing methodology

The simplest way to determine the stabilization area (Fig. 4) is to make a *F-N* dependency diagram. The stabilization area is defined by the beginning (N_{bs}) and the end of stabilization (N_{es}). The failure cycle (N_f) defined by the standard [1, 2] is read from the *F-N* diagram, which defines the characteristic stabilized hysteresis $N_s = N_{f/2}$. The characteristic stabilized hysteresis N_s is the data diagram $\Delta\varepsilon$-ΔF for the cycle N_s (Fig. 4b).

A result of low-cycle fatigue testing on one test specimen (one amplitude strain level) is the record in EXCEL (Fig.5a *(Record of data in Excel of testing of NN-70 steel for amplitude strain level, $\Delta\varepsilon/2\approx0.80\%$)*), which can be further processed according to requirements using the available tools in EXCEL. Tables 2 [21] and 3 and Fig. 6 and Fig. 7 [21] were derived from this processing.

The results were processed as follows:

1. Only maximum load values for each amplitude level are selected (Fig. 5b *(Extraction of data values of max load forces of LCF test)* and Fig. 5c *(Extracted values of max load data of LCF steel NN-70 for amplitude strain level, $\Delta\varepsilon/2\approx0.80$ %)*).
2. A diagram, as in Figure 5d *(Making diagrams of max load forces - number of cycles)*, was made from the values F_{max} of the number of cycles (maximum number and maximum load forces (force [kN]). It can be seen that in the range between 100 and 150 cycles the curve is almost linear, so its linearity is determined in a given range (Fig.5e *(Linearization of data max load force – number of cycles in the obvious stabilization range)*). The value of R^2 (R^2 - coefficient of determination) is low, the range is expanded towards the lower and higher number of cycles until the maximum value of R^2 is obtained. In this example, it is the cycle range between $N_{ps} = 33 = N_{bs}$ (Fig. 5f,g *(Determination of the stabilization start cycle, $N_{bs}=N_{ps}$, for max value R^2)* and $N_{ks} = 184 = N_{es}$, (Fig. 5h,i *(Determination of the stabilization end cycle, $N_{es}=N_{ks}$, for max value R^2)*).
3. Based on a certain linearity, we calculated the maximum value of load forces for each cycle based on the obtained formula. A diagram, as in Fig. 5j (point 1 in the Figure) *(Calculated max load values for each LCF test cycle)*, was made from the values of the number of cycles and the calculated values of maximum load forces.
4. In the next step, the diagrams obtained as described in points 2 and 3 are overlapped (the diagram from point 3 is copied to the diagram from point 2) (see Fig.5j *(Calculated max load values for each LCF test cycle)*).
5. The N_f cycle is defined by the ISO 12106: 2017 (E) [1] standard and represents the cycle in which significant damage to the LCF specimen occurred and is determined as

shown in Fig. 5k *(Determination of failure cycle, N_f and characteristic stabilization cycle, N_s)*, $N_f = 208$. The 0.75 values F_{max} of maximum force in the N_{es} cycle were calculated and the minimum difference between the maximum value of force and the 0.75 value of maximum force for cycles larger than N_{es} cycle is required. The cycle of the stabilization curve $N_s = N_{f/2} = 104$ is a representative cycle used to read data for the construction of LCF curves (CSSC and BCLCF, Fig. 4c and 4d) and is shown in Fig.5k *(Determination of the value of the characteristic stabilization cycle, N_s)*.

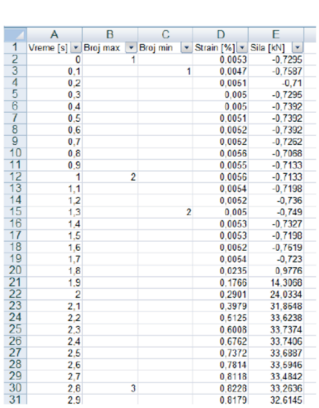

a)

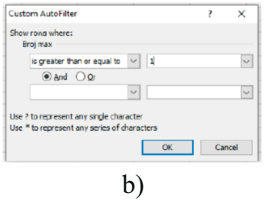

b)

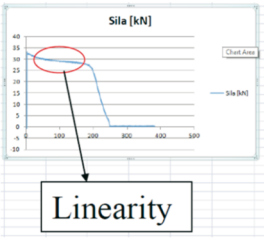

d)

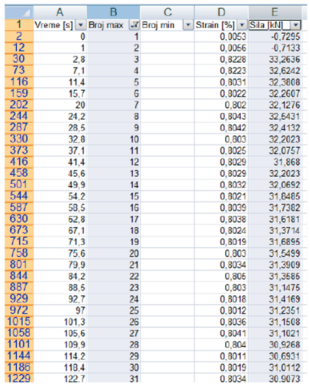

c)

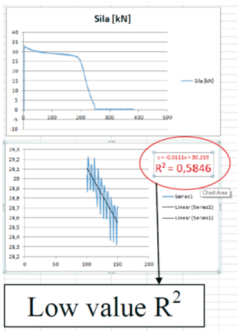

e)

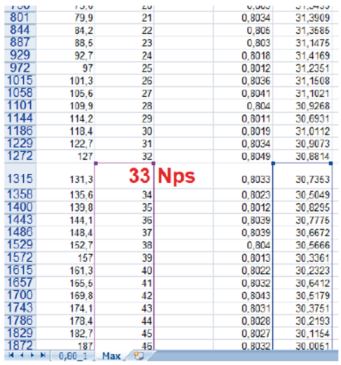

f)

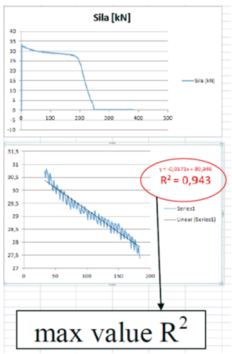

g)

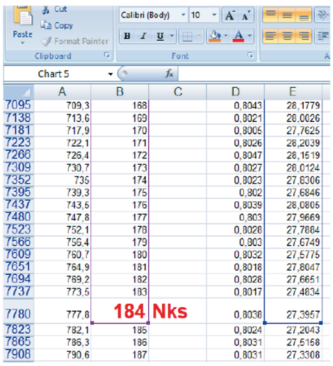

h)

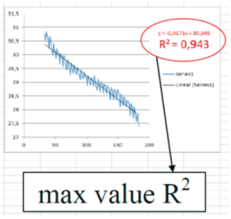

i)

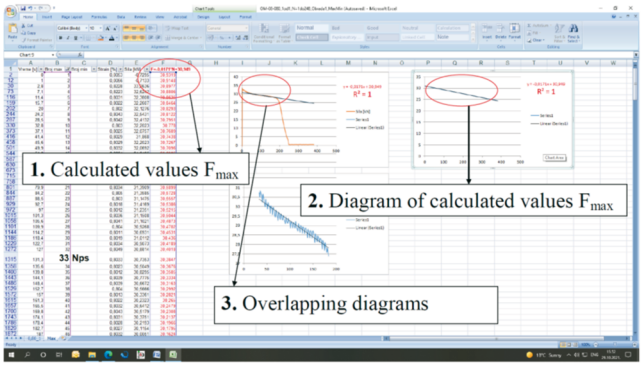

j)

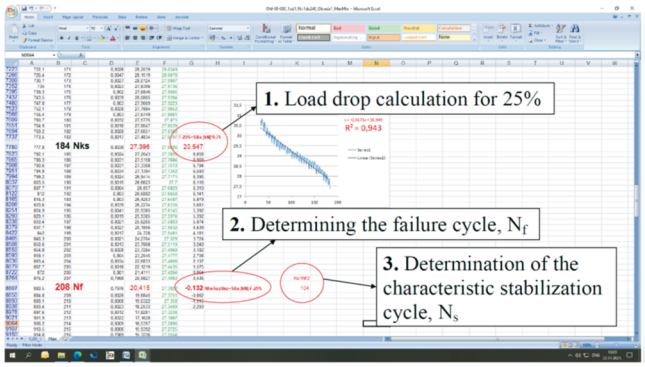

k)

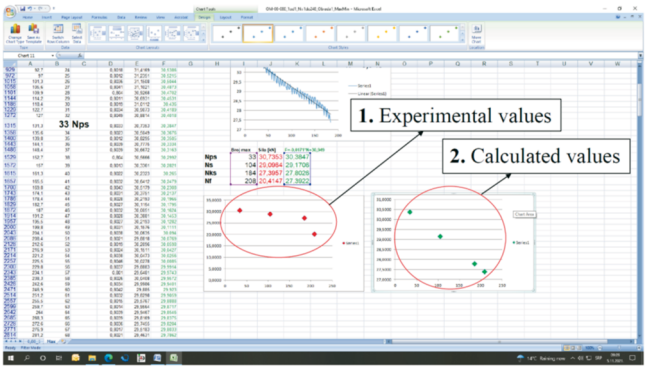

l)

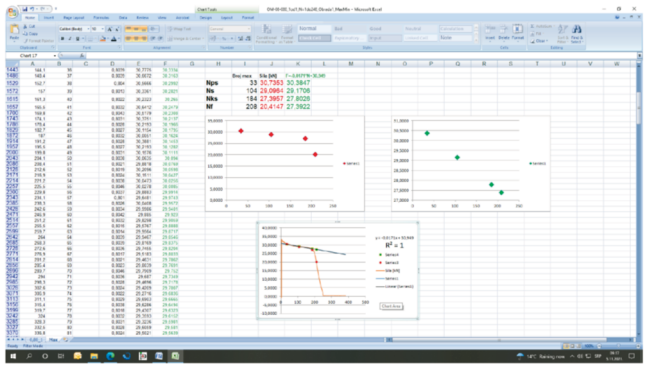

m)

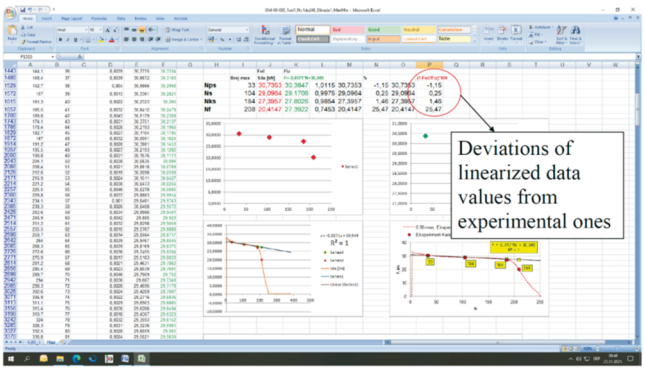

n)

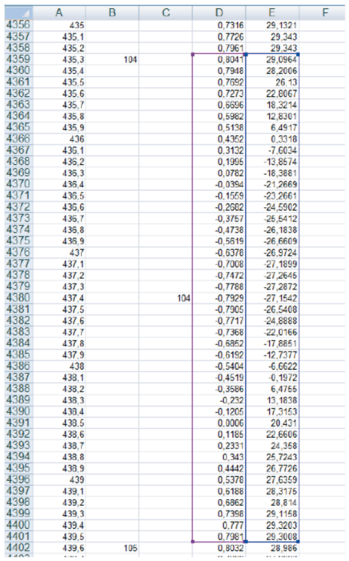

o)

Fig. 5 Screenshots of the new methodology for data processing after LCF steel testing

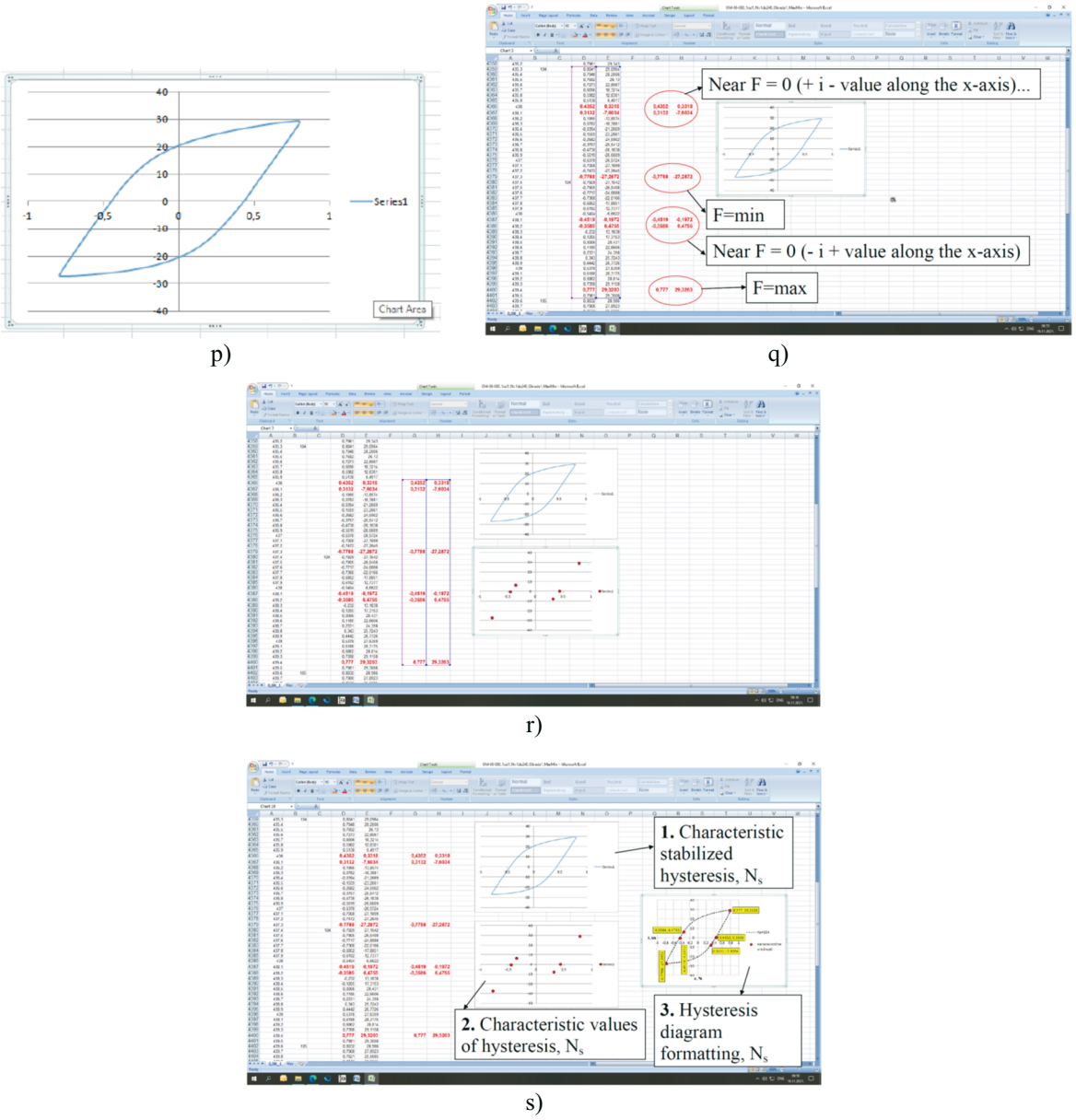

p) q)

r)

s)

Fig. 5 Screenshots of the new methodology for data processing after LCF steel testing (continued)

6. Diagrams were established from the values F_{max} of $N_{ps} = N_{bs}$, N_s, $N_{ks} = N_{es}$ and N_f (Fig. 5l *(Diagrams of values of max load forces (experimental and calculated) for characteristic cycles)*), which are merged with the diagram from point 2 (Fig. 5m *(Merging all diagrams)*).
7. In the next step, the diagrams of Fig. 5n *(Linearization of the maximum load force of the specimen in the LCF test for the amplitude strain level $\Delta\varepsilon/2\approx0.80\%$ and deviations from the experimental values of the max load force)* were formatted, and the deviations in relation to the read loads were calculated.
8. When the characteristic stabilized hysteresis, N_s, was determined, a diagram was constructed from the original test data (Fig. 5o, and Fig. 5p *(Diagram of characteristic stabilized hysteresis in the N_s cycle)*).
9. Maximum and minimum values of load F as well as values close to load $F = 0$ were extracted from the data (+ i - values along the x axis, needed to determine $\Delta\varepsilon_p/2$ and $\Delta\varepsilon_e/2$) (Fig.5q *(Extraction of values F = max; min; + - along the x-axis and - + along*

the x-axis for the N_s cycle)). Finally, a diagram was constructed (see Fig.5r *(Constructing a diagram of the value of F = max; min; + - along the x-axis and - + along the x-axis for the N_s cycle)*).

10. At the end, the diagrams from points 8 and 9 were merged into one diagram (Fig.5s *(Merging the N_s diagram into a single diagram for further processing)*), which is formatted to serve for further data processing for the purpose of defining characteristic low-cycle fatigue curves (Fig. 4c and Fig. 4d).

5. Results of data processing of LCF steel testing with a new methodology

From the diagram of the dependence of the number of cycles and the calculated load based on the linearization formulas for the area of stabilized cycles, from N_{bs} to N_{es}, for all amplitude strain levels, a unique diagram was constructed showing the load behaviour for all strain ranges in which the given steel was tested with low cyclic fatigue (Fig. 6).

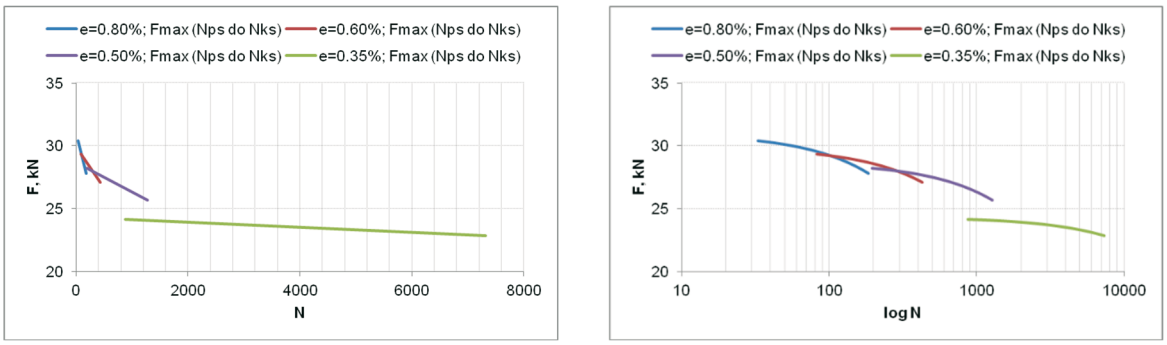

Fig. 6 Behaviour of maximum calculated load for the area of stabilized cycles, from N_{bs}=N_{ps} to N_{es}=N_{ks} for all LCF tested amplitude strain levels in the normal and logarithmic distribution of the number of cycles

Figures 7 a and b show the maximum and minimum values of the specimen load during the N cycle of exposure to low-cycle fatigue. In Fig. 7 c, d, e and f, a linear dependence of the maximum values of the load (so-called stabilization area) was established and the characteristic hysteresis cycles of the beginning of stabilization, N_{bs}, end of stabilization, N_{es}, and the so-called characteristic stabilization cycle, N_s (defined by standard [1]) from which all other characteristics of LCF steel for a given amplitude strain level are determined. The cycle of significant specimen damage, N_f (defined by standard [1]) was also determined. From the graphic part of Fig. 6, Table 2 is created.

Table 2 Characteristic processed test data of LCF steel NN-70

LCF NN-70		Stabilization area		Characteristic cycles			
Specimen	$\Delta\varepsilon$/2,%	y=F, kN; x=N	R^2	N_{bs}	N_{es}	N_f	N_s= N_f/2
09	0.35	F=-0.0002N+24.319	0.9584	875	7315	8337	4169
03	0.50	F=-0.0023N+28.659	0.9663	195	1281	1403	702
06	0.60	F=-0.0064N+29.859	0.9496	83	426	504	252
08	0.80	F=-0.0171N+30.949	0.9430	33	184	208	104

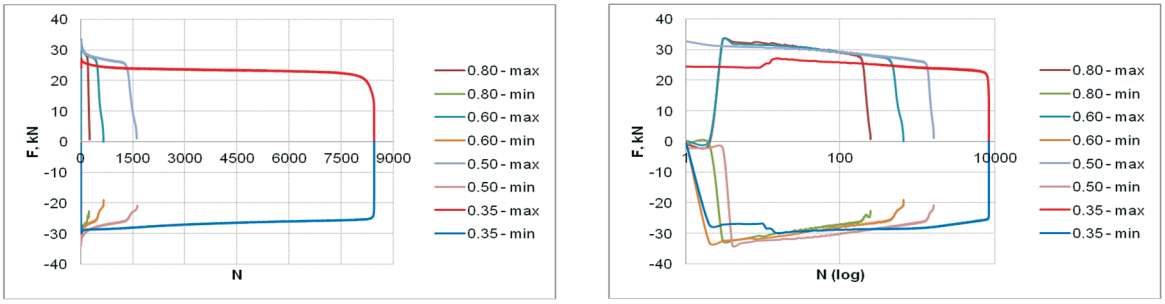

a) b)

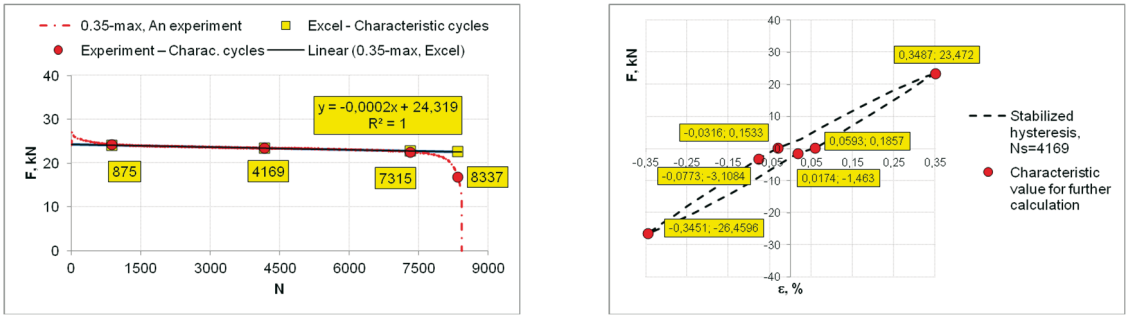

c) specimen 09, $\Delta\varepsilon/2 \approx 0.35$ %

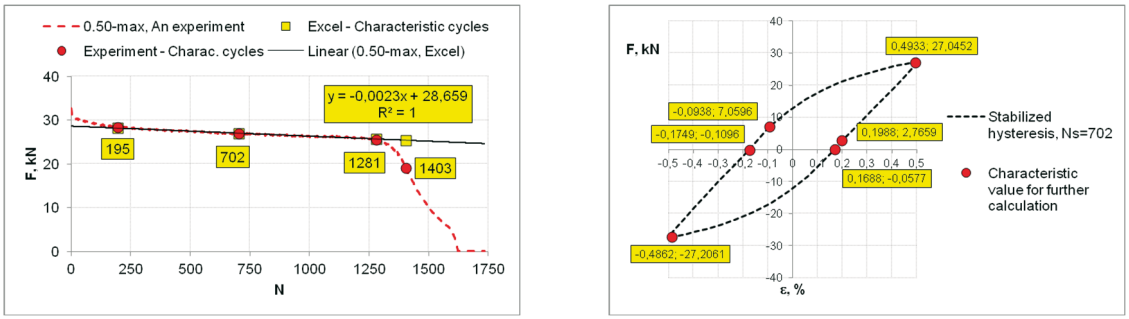

d) specimen 03, $\Delta\varepsilon/2 \approx 0.50$ %

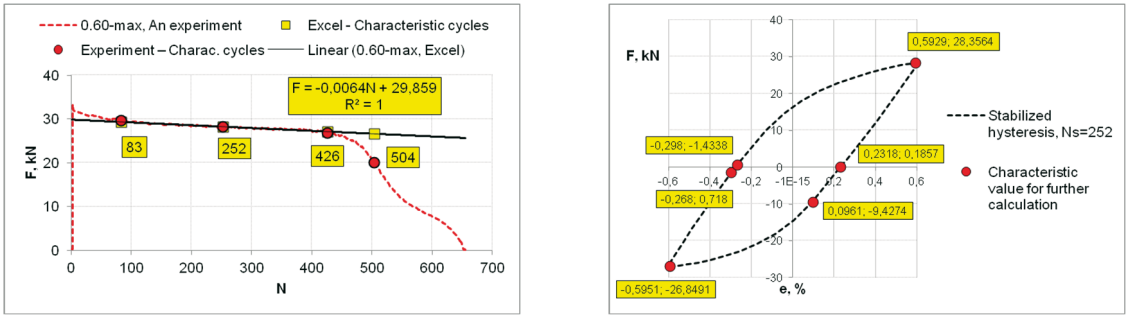

e) specimen 06, $\Delta\varepsilon/2 \approx 0.60$ %

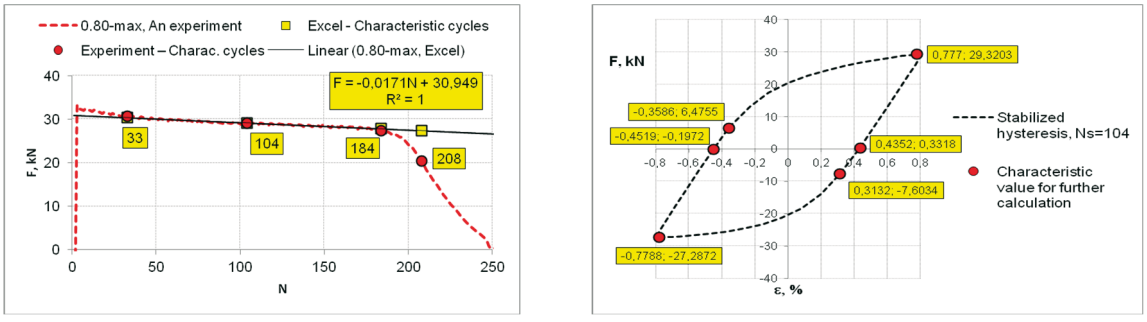

f) specimen 08, $\Delta\varepsilon/2 \approx 0.80$ %

Fig. 7 Graphical processing of LCF base metal (BM) test results, NN-70 steel

Table 3 shows the results of the fast calculation of the maximum load in the stabilization area and the results obtained by the slow search and reading of LCF test data from a specific hysteresis for a certain load cycle.

Table 3 Calculated and read data of max. load in the stabilization area during testing of LCF steel NN-70

LCF NN-70		Calculated data (Cd)				Read data (Rd)	Deviation of F_{Cd} from F_{Rd}
Specimen	$\Delta\varepsilon/2$, %	Load cycle		y=F, kN; x=N	F_{Cd}, kN	F_{Rd}, kN	$(1-F_{Rd}/F_{Cd})\cdot 100$, %
09	0.35	N_{bs}	875	F=-0.0002N+24.319	24.1440	24.3320	-0.78
		N_s	4169		23.4852	23.4720	0.06
		N_{es}	7315		22.8560	22.5665	1.27
03	0.50	N_{bs}	195	F=-0.0023N+28.659	28.2105	28.3824	-0.61
		N_s	702		27.0444	26.9446	0.37
		N_{es}	1281		25.7127	25.6172	0.37
06	0.60	N_{bs}	83	F=-0.0064N+29.859	29.3278	29.5897	-0.89
		N_s	252		28.2462	28.2461	0.00
		N_{es}	426		27.1326	26.8408	1.08
08	0.80	N_{bs}	33	F=-0.0171N+30.949	30.3847	30.7353	-1.15
		N_s	104		29.1706	29.0964	0.25
		N_{es}	184		27.8026	27.3957	1.46

6. Conclusion

This paper defines a new data processing methodology obtained after LCF steel testing. It allows for the rapid determination of characteristic stabilized hysteresis, Ns, from data obtained by the LCF testing of steel for each amplitude level of regulated strain. The new methodology of data processing after the LCF testing of steel avoids the problem of objective and subjective influence in determining stabilized hysteresis. All the data used to define the characteristic curves of low-cycle fatigue are mathematically determined from the LCF test data, so there is practically no objective or subjective influence. In addition, the new post-LCF data processing methodology enables the rapid calculation of the approximate maximum load force for any stabilization cycle according to certain formulas obtained from the LCF test data. If the exact value of the maximum load is required, this is read from the test results for a specific load cycle. The presented new data processing methodology after the LCF testing of steel is also applicable to the LCF testing of other structural materials. Deviation of the values obtained by this approximate method is no higher than -1.15% and + 1.46% (see Table 3).

Acknowledgement

This research is supported by the Ministry of Education, Science and Technological Development of the Republic of Serbia (Contract No. 451-03-68/2022-14/ 200012).

REFERENCES

[1] ISO 12106:2003(E) Metallic materials-fatigue testing-axial-strain-controlled method, *Geneva: ISO* **2003**

[2] ASTM E606-04 Standard practice for strain-controlled fatigue testing, *ASTM International, West Conshohocken, Pennsylvania, USA*, **2004**.

[3] Posavljak S. Naponsko-deformaciona analiza i zamor materijala rotacionih diskova turbomlaznih motora, *Master's thesis, University of Belgrade, Faculty of Mechanical Engineering*, **1999**.

[4] Posavljak S. Istraživanje zamornog veka rotacionih diskova avionskih motora, *Doctoral dissertation, University of Belgrade, Faculty of Mechanical Engineering*, **2008**.

[5] Schijve J. Fatigue of Structures and Materials, *Kluwer Academic Publishers, New York, Boston, Dordrecht, London, Moscow*, **2004**.

[6] Bannantine J. A.; Comer J.; Handrock J. Fundamentals of Material Fatigue Analysis, *Prentice-Hall, Englewood Clifs, New Jersey,* **1990**.

[7] Janković D. M. Malociklusni zamor, *University of Belgrade, Faculty of Mechanical Engineering*, **2001**.

[8] Janković D. M. Eksperimentalno određivanje tokova zamaranja materijala pri ciklično promenljivim elasto-plastičnim deformacijama, *Doctoral dissertation, University of Belgrade, Faculty of Mechanical Engineering*, **1988**.

[9] Aleksić V. Low cycle fatigue of high strength low alloy steels, *Doctoral dissertation, University of Belgrade, Faculty of Technology and Metallurgy*, **2019**.

[10] Aleksić V.; Aleksić B.; Milović Lj. Methodology for determining the region of stabiliyation of low-cycle fatigue, *16th International Conference on New Trends in Fatigue and Fracture (NT2F16), May 24-27, Dubrovnik, Croatia,* **2016**, 189 – 190.

[11] Aleksić V.; Milović Lj.; Aleksić B.; Hemer A.M. Indicators of HSLA steel behavior under low cycle fatigue loading, *21st European Conference on Fracture, ECF21, 20-24 June 2016, Catania, Italy, Procedia Structural Integrity 2*, **2016**, 3313–3321. https://doi.org/10.1016/j.prostr.2016.06.413

[12] Aleksić V.; Aleksić B.; Milović Lj. Metodologija određivanja pokazatelja ponašanja HSLA čelika pri delovanju niskocikličnog zamora, *V Međunarodni kongres „Inženjerstvo, ekologija i materijali u procesnoj industriji", Jahorina, BiH, 15.03.-17.03.* **2017**, 1123-1135.

[13] Aleksić V. et al., Behaviour of Nionikral-70 in low-cycle fatigue, *Structural Integrity and Life, Vol.17, No 1*, **2017**, 61-73.

[14] Aleksić B. et al. Determination of the region of stabilization on low-cycle fatigue HSLA steel from test data, *In: Proceedings of the 17th International Conference on New, Trends in Fatigue and Fracture, Springer*, **2018**, 101-113. https://doi.org/10.1007/978-3-319-70365-7_12

[15] Aleksić V. et al. Effect of LCF on behavior and microstructure of microalloyed HSLA steel and its simulated CGHAZ, *Engineering Failure Analysis, Vol. 104*, **2019**, 1094-1106. https://doi.org/10.1016/j.engfailanal.2019.06.017

[16] Milović, LJ.; Bulatović, S.; Aleksić, V.; Burzić, Z. Low cycle fatigue of weldments produced of a high strength low alloyed steel, *Procedia Materials Science, 3:* **2014**, 1429-1434. https://doi.org/10.1016/j.mspro.2014.06.231

[17] Bulatović S. Elastic-plastic behavior of welded joint of high strength low alloy in conditions of low cycle fatigue, *Doctoral dissertation, University of Belgrade, Faculty of Mechanical Engineering*, **2014**.

[18] Bulatovic S.; Burzic Z.; Aleksic V.; Sedmak A.; Milovic Lj. Impact of choice of stabilized hysteresis loop on the end result of investigation of high-strength low-alloy (HSLA) steel on low cycle fatigue, *Metalurgija, 53,* 4, **2014**, 477-480.

[19] Bulatovic S.; Milovic Lj.; Sedmak A.; Samardžić I. Identification of low cycle fatigue parameters of high strength low-alloy (HSLA) steel at room temperature, *Metalurgija, 53, 4*, **2014**, 466-468.

[20] Aleksić B. et al. Numerical simulation of fatigue crack propagation: A case study of defected steam pipeline, *Engineering Failure Analysis, Vol. 106*, **2019**. https://doi.org/10.1016/j.engfailanal.2019.104165

[21] Aleksić V.; Milović Lj.; Bulatović S.; Zečević B.; Maksimović A. Chapter 32, Chapter Title: Determination of LCF Plastic and Elastic Strain Components of Steel, *Book: Machine and Industrial Design in Mechanical Engineering,* **2022**, https://doi.org/10.1007/978-3-030-88465-9

[22] Kubit A.; Jurczak W.; Trzepiecinski T.; Faes K. Experimental and Numerical Investigation of Impact Resistance of Riveted and RFSSW Stringer-Stiffened Panels in Blunt Impact Tests, *Transactions of FAMENA XLIV-3* (**2020**), 47-58. https://doi.org/10.21278/TOF.44304

[23] Furch J. The Model Prediction of Life Cycle Ownership Costs of Special Motor Vehicles, *Transactions of FAMENA XLIV-4* (**2020**), 99-114. https://doi.org/10.21278/TOF.444004719

[24] Zhang J.; Gan J.; Zeng Y. Application of a Probability Model Based on Paris' Low in Assessing Fatigue Life of Marine High-Strength Steel Structures, *Transactions of FAMENA XLV-2* (**2021**), 89-100. https://doi.org/10.21278/TOF.452015320

[25] Socie D. F.; Mitchell M. R.; Caulfield E. M. Fundamentals of modern fatigue analysis, *FCP Report No. 26, Department of Theoretical and Applied Mechanics, A report of the fatigue control program, College of Engineering, University of Illinois, Urbana, USA*, **1978**.

Submitted: 12.4.2022

Accepted: 09.11.2022

Vujadin Aleksić
vujadin.aleksic@institutims.rs
Srđan Bulatović*
Institute for Materials Testing-IMS,
Bulevar vojvode Mišića 43, Belgrade,
Serbia
Bojana Zečević
baleksic@tmf.bg.ac.rs
Ana Maksimović,
aprodanovic@tmf.bg.ac.rs
University of Belgrade, Innovation Centre
of Faculty of Technology and Metallurgy,
Karnegijeva 4, Belgrade, Serbia
Ljubica Milović
acibulj@tmf.bg.ac.rs
University of Belgrade, Faculty of
Technology and Metallurgy,
Karnegijeva 4, Belgrade, Serbia
*Corresponding author:
srdjan.bulatovic@institutims.rs